View metadata, citation and similar papers at core.ac.uk
brought to you by CORE
provided by Chalmers Publication Library

Cite this: DOI: 10.1039/c2sm26394g
www.rsc.org/softmatter

COMMUNICATION

Formation of giant unilamellar vesicles from spin-coated lipid films by localized IR heating†

Céline Billerit, Gavin D. M. Jeffries, Owe Orwar and Aldo Jesorka*

Received 15th June 2012, Accepted 23rd August 2012
DOI: 10.1039/c2sm26394g

Published on 13 September 2012 on http://pubs.rsc.org | doi:10.1039/C2SM26394G
Downloaded by Chalmers Tekniska Hogskola on 17 September 2012

We report a novel method for the generation of GUVs (generate unilamellar vesicles) from spin-coated lipid films by means of localized heating. This technique enables GUV formation from both charged and neutral lipid species, as well as from a complex lipid mixture, in various ionic strength conditions. Encapsulation was possible during and after GUV formation.

Giant unilamellar vesicles (GUVs) are useful models for the study of cellular membranes, with similar size and composition to biological cells, which can be directly observed and manipulated using light microscopy. Due to their biomimetic properties, GUVs have particular utility for the study of lateral lipid heterogeneities,[1] membrane budding and fusion,[2,3] and in the construction of protocells.[4]

Several methods are employed for GUV formation including electroformation,[5,6] gentle hydration,[7,8] interdigitation-fusion,[9] emulsion-based methods,[10,11] and more recently using microfluidic devices.[12,13] These methods generate GUVs, but have a limited scope for variations in lipid composition and ionic strength conditions, or they require special equipment and microfabrication expertise.

Herein we report a new, superior GUV formation method starting with spin-coated lipid films. An IR-B laser, previously utilized for the thermal modification of multilamellar vesicles (MLVs),[14] is applied to locally heat planar lipid deposits, rapidly transforming them into GUVs. This method is advantageous as: (i) it uses affordable off-the-shelf equipment, (ii) it produces vesicles from charged or uncharged lipids under different ionic conditions, (iii) it allows for the encapsulation of molecules into the formed or forming vesicles. We successfully generated vesicles from a single lipid species as well as from a mixture of lipids, in both low and high ionic strength conditions, and demonstrate that the GUVs formed by this procedure are structurally similar to vesicles generated by established methods.

We found that the lamellar distribution obtained by our methodology, which was assessed using fluorescence intensity measurements, is comparable to that obtained using the dehydration–rehydration technique. We also investigated the formation of transient pores in the bilayers, enabling encapsulation of compounds inside the vesicles, through use of the crowding agent dextran. Additionally, we demonstrated the creation and efficient employment of spin-coated lipid surfaces to control the molecular composition of the vesicles, as well as the surrounding environment.

Lipid films were prepared on SiO_2 surfaces by employing the spin-coated method detailed by Estes and Mayer.[15] A poly(dimethylsiloxane) (PDMS) frame was placed onto the lipid spin-coated surface to form a chamber (Fig. 1A). The chamber was filled with 60 mM ionic strength phosphate buffered saline (PBS) solution to hydrate the lipid film. Immediately following hydration, the targeted location was

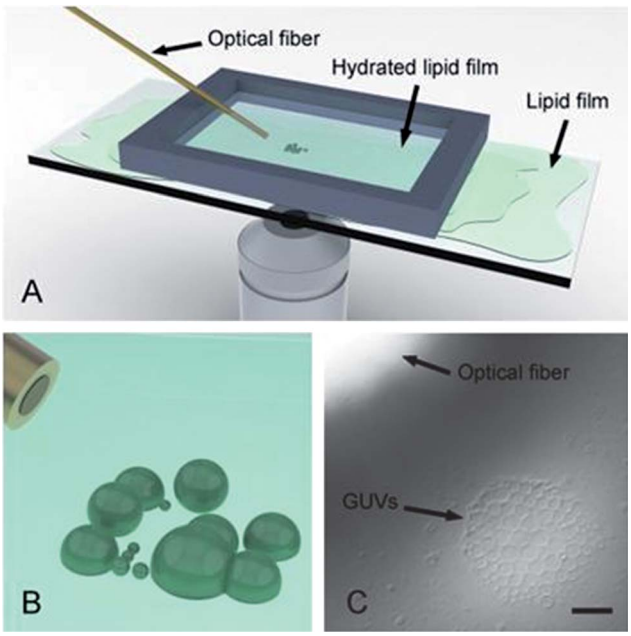

Fig. 1 Schematic diagram of the setup used for the generation of GUVs from a deposited lipid film. Using an IR-B laser, directed through an optical fiber, the sample is heated, driving the formation and release of vesicles. (A) and (B) illustrate a typical setup where the fiber is positioned and directed towards the surface inside a well of hydrating medium. Spherical vesicles can be seen to form at the chosen location. (C) A differential interference contrast (DIC) image of GUV formation from a POPC lipid film during heating. The spin-coated lipid film was hydrated with 60 mM ionic strength PBS solution. Vesicle formation can be observed relative to the optical fiber. The scale bar represents 20 μm. The DIC image was recorded using a 40×/1.25 NA objective and a high-resolution camera.

Department of Chemical and Biological Engineering, Chalmers University of Technology, SE-412 96, Göteborg, Sweden. E-mail: aldo@chalmers.se
† Electronic supplementary information (ESI) available: Materials and methods and supporting figures. See DOI: 10.1039/c2sm26394g

Published on 13 September 2012 on http://pubs.rsc.org | doi:10.1039/C2SM26394G
Downloaded by Chalmers Tekniska Hogskola on 17 September 2012

locally heated using an IR-B laser directed through an optical fiber (Fig. 1B). Multiple vesicles were formed within a few seconds, however, the heating was maintained for several minutes until the vesicles had grown to a sufficiently large size (~2–10 μm diameter) (Fig. 1C). The stability of the vesicles was confirmed by observation 30 minutes after formation (Fig. S1 in the ESI†).

To confirm the use of this technique as an easily deployable vesicle formation strategy, we investigated the effects of lipid composition, buffer ionic strength, and the encapsulation ability. We used three zwitterionic lipids which exhibit different main phase transition temperatures (T_m), 1-stearoyl-2-arachidonoyl-*sn-glycero*-3-phosphoethanolamine (PE), 1-palmitoyl-2-oleoyl-*sn-glycero*-3-phosphocholine (POPC), 1,2-dimyristoyl-*sn-glycero*-3-phosphocholine (DMPC). Their T_m values are respectively, 32 °C for PE, 23 °C for DMPC and −2 °C for POPC.[16–18] For each composition, we successfully generated vesicles using the same heating protocol, employing a local temperature range which was empirically measured to be between 80 and 90 °C (Fig. 1C and 2A-B), well above the liquid crystalline phase transition temperature for the respective lipid compositions. The ability to form GUVs by means of the gentle hydration method is strongly correlated with the liquid crystalline phase.[19] After hydration, the lipid films swell, then due to thermal fluctuations, the outermost bilayer begins to separate from the surface, initiating the formation of vesicles. In the gel phase, the lipid bilayers remain stacked inhibiting GUV formation. We applied the technique using two negatively charged lipid compositions, 1,2-dioleoyl-*sn-glycero*-3-phospho-L-serine (DOPS) and soybean polar lipid extract (SPE), to form GUVs (Fig. 2C-D). The complexity of the SPE membrane, coupled with the incomplete understanding of the thermotropic behaviour of its individual components, make it difficult to determine the SPE lipid film morphology at 80 °C. On the other hand, DOPS exhibits a T_m at −11 °C,[20] resulting in a liquid crystalline phase at 80 °C. GUV formation, from a positively charged lipid composition, 1,2-dioleoyl-3-trimethylammonium-propane (DOTAP), was also performed (Fig. S2 in the ESI†).

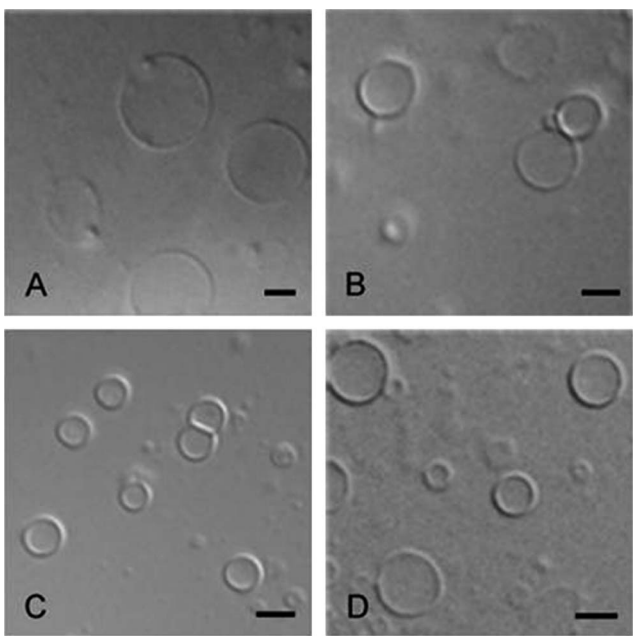

Fig. 2 DIC images of GUVs from different lipid types, formed by means of localized heating. (A) GUVs from PE. (B) GUVs from DMPC. (C) GUVs from DOPS. (D) GUVs from SPE. The scale bars represent 5 μm. The DIC images were recorded by using a 40×/1.25 NA objective and a high-resolution camera.

To confirm the formation of free vesicles, axial imaging (XZ), was utilized, to discriminate between vesicles and membrane blisters (hemispherical swollen sections of the membrane appearing as spherical objects when viewed laterally). We investigated the morphological change of hydrated lipid films during thermal treatment, through utilization of rapid XZ scanning, achieving axial or surface orthogonal views. An SPE lipid film was prepared containing 1% 1,2-dihexadecanoyl-*sn-glycero*-3-phosphoethanolamine (Texas Red DHPE), to facilitate membrane visualisation. Fig. 3A shows vesicles forming during the heating, while Fig. 3B shows a vesicle formed after heating. The XZ laser scanning micrographs demonstrate the formation of small vesicles, which increase in size and then detach from the surface (Fig. 3B). These results confirm that we are able to generate spherical GUVs, which are released into the solution and completely detached from the lipid film. The progressive growth during heating was confirmed *via* lateral (XY) imaging, of a single vesicle (Fig. S3 in ESI†).

The ionic strength of the hydrating medium also plays an important role during vesicle formation, imparting osmotic pressure to the system. Typical formation conditions utilize a 60 mM ionic strength PBS solution, however a 140 mM PBS solution was also tested to better reproduce physiological conditions. GUVs with diameters ranging between 2 and 10 μm were able to be formed under both conditions (Fig. S5 in the ESI†).

Another key parameter for practical vesicle preparation schemes is encapsulation, whereby we implemented two different approaches; solute addition to the medium during, or after, vesicle formation. One minimally intrusive method of achieving encapsulation is through the use of a macromolecular crowding agent.[21] One such agent, dextran, attached to solutes, has been reported to enable easier encapsulation during vesicle formation.[22] As before, the membrane was visualised using 1% Texas Red DHPE. This lipid film was hydrated using a 60 mM ionic strength PBS solution, containing 0.02 mg mL^{-1} of dextran-labeled fluorescein isothiocyanate (FITC-dextran), prior to the vesicle formation. Separate micrographs of the red (Texas Red

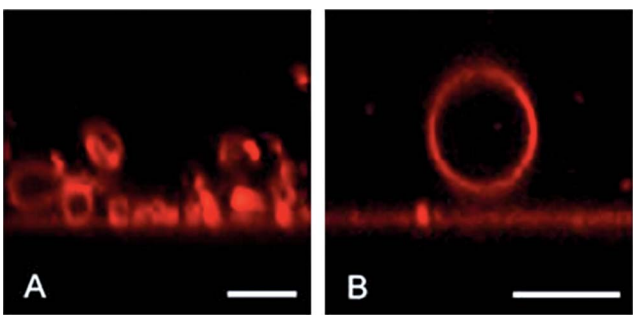

Fig. 3 Forming/formed vesicles during the heating process. XZ confocal laser scanning micrographs of vesicles generated from a mixture of 99% SPE and 1% Texas Red DHPE. (A) Forming vesicles being released from the surface during heating. Optical distortions are apparent due to motion of the vesicles during the imaging, resulting from the heating. (B) A vesicle formed and detached from the surface after heating. The scale bars represent 10 μm. A 3D reconstruction of a similar vesicle is shown in the ESI (Fig. S4†).

This journal is © The Royal Society of Chemistry 2012

Published on 13 September 2012 on http://pubs.rsc.org | doi:10.1039/C2SM26394G
Downloaded by Chalmers Tekniska Hogskola on 17 September 2012

DHPE) and green (FITC-dextran) channels are shown in Fig. 4A–D. Both low and high encapsulation efficiencies of FITC-dextran into the vesicles can be observed for the same sample. This variance is likely based upon the transient pore formation mechanism for encapsulation. It is known that membrane permeability increases with temperature.[23] The reason for this increase is the enhanced area fluctuations that lead to a maximum in the lateral compressibility. Nagle and Scott,[24] proposed that changes in lateral compressibility can lead to the facilitation of pore formation, since the increased compressibility lowers the work necessary to create a membrane defect.

To support this hypothesis, we performed the same experiment by adding FITC–dextran both directly after vesicle formation as well as 30 minutes after formation. Introduction immediately after formation, as with inclusion into the hydration medium, led to the encapsulation of FITC–dextran into the vesicles with various efficiencies (Fig. 4E–H). On the contrary, half an hour after vesicle formation, no encapsulation was observed (data not shown). These results are consistent with the assumption of transient pore formation. Indeed, we successfully demonstrated the feasibility of encapsulating bioactive molecules inside vesicles. The simplest way to avoid thermal degradation was to utilize post formation introduction to the medium.

We further investigated the use of dextran as an encapsulation promotion agent (unconjugated to the solute) during vesicle formation, by addition of both fluorescein and dextran individually to the PBS solution. An encapsulation efficiency of 0.77 ± 0.10 ($n = 100$) was obtained, similar to 0.79 ± 0.18 ($n = 100$) found in the FITC–dextran conjugated experiments (Fig. S7 in the ESI†). Encapsulation of fluorescein alone, without the addition of dextran, was not possible. These results suggest that transient pores, formed within the membrane, are stabilized by dextran, allowing the influx/efflux of molecules. Although it has been shown that addition of polymers such as dextran, has an impact on a number of processes with biological importance,[25,26] the effect on pore dynamics still remains uncertain. Our findings suggest that in the presence of dextran, transient pores remain open for longer, allowing encapsulation of molecules into the vesicle during and after heating.

It has been previously discussed that a distribution of vesicle lamellarities occurs when global generation techniques are employed.[27] Analysis of vesicle lamellarity from such techniques was investigated utilizing fluorescence measurements of the membrane. This technique was employed for the study of vesicles generated by IR laser radiation, compared to those formed by the commonly used dehydration–rehydration technique.[28] In total 50 vesicles were analyzed; 25 formed by localized heating and 25 formed by dehydration–rehydration, the membranes of which were visualised by incorporating 1% of Texas Red DHPE. Images were obtained using laser scanning confocal microscopy, while maintaining the fluorescent excitation intensity and the confocal acquisition settings, for all the vesicles under observation. A typical example of this fluorescence measurement is highlighted in the ESI (Fig. S8†). Through intensity analysis, and subsequent subtraction of the background directly surrounding the vesicle, an accurate value for the membrane intensity could be measured. Using the analysis scheme presented by Akashi *et al.*,[27] we observed a distribution of lamellarity in the formed vesicles. The measured distribution was found to be almost identical for

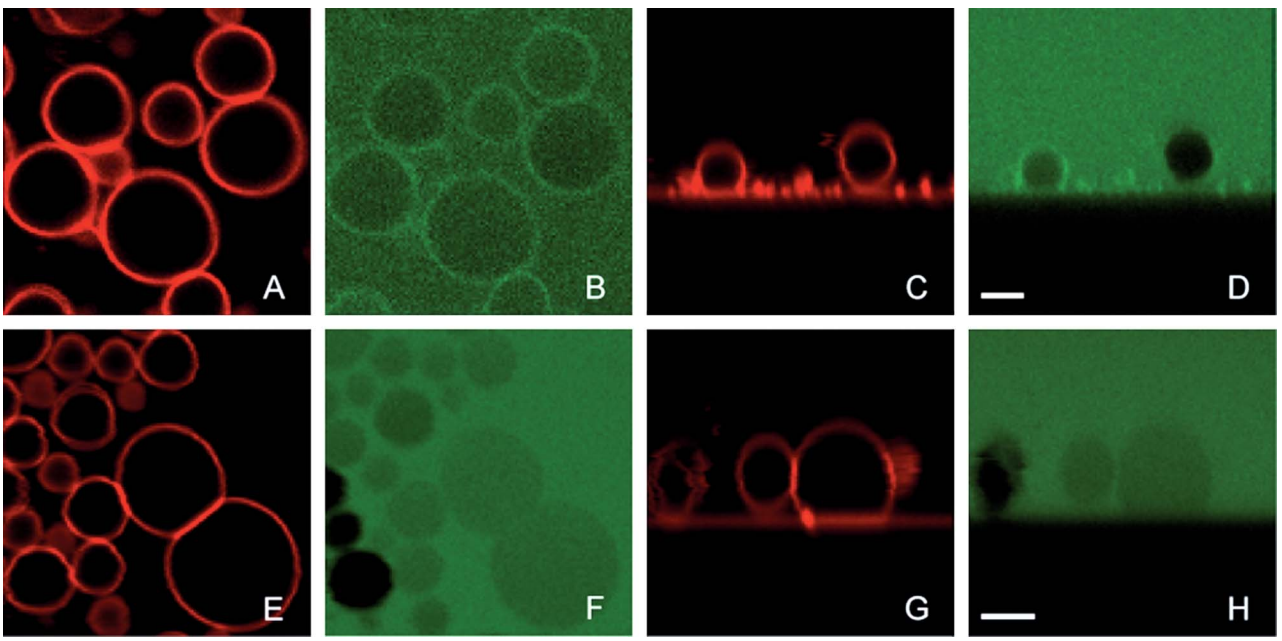

Fig. 4 Confocal laser scanning micrographs of forming/formed vesicles from 99% SPE and 1% Texas Red DHPE, during encapsulation of FITC–dextran. (A–D) Display encapsulation variations 'during' the formation procedure. Separate XY and XZ confocal laser scanning micrographs are shown in A and B, and C and D respectively. The scale bar in (D) represents 5 μm, and is valid for (A–D). (E–H) Display encapsulation variations in 'formed' vesicles. Separate XY and XZ confocal laser scanning micrographs are shown in E and F and G and H respectively. The scale bar in (H) represents 5 μm, and is valid for (E–H). (A, C, E and G) Show the membrane dye Texas Red DHPE whereas (B, D, F and H) show the encapsulated FITC–dextran. The pinhole was reduced to 0.25 Airy units, to effectively remove contributions from out of focus fluorescence in the solution, making exchange of the external solution prior to measurement unnecessary. Variations in fluorescence intensity within the vesicles therefore represent the variation in encapsulation.

both vesicles formed by heating and by dehydration–rehydration (Fig. S9 in ESI†), indicating that generation by the heating technique does not significantly influence the lamellarity distribution. Moreover, this lamellarity distribution would probably account for the variance in encapsulation yields. It would be expected that transient pores in unilamellar membranes allow high efficiency encapsulation, while bi- or tri-lamellar membranes restrict passage to the interior of the vesicle, severely limiting the encapsulation.

To test the versatility of this approach, the stability of spin-coated lipid films, for dry storage and subsequent use, was studied. We stored spin-coated lipid film surfaces for 1 to 30 days. DIC images of GUVs formed after 1, 3, 7 and 30 days of storage can be found in the ESI (Fig. S10†). We observed no significant alteration in either the size or number of vesicles created, for storage times of up to 1 month. This allows for convenient on-demand generation of GUVs from pre-prepared surfaces.

In conclusion, we have presented a rapid on-demand method for generation of GUVs from spin-coated lipid films, by means of localized heating, with the ability to encapsulate molecules. This simple technique employs a 1470 nm laser, guided by a positioned optical fiber. Neither specialized chambers, nor lipid specific setup adjustments, are required for vesicle formation. This technique enables GUV formation from charged and neutral single lipid species, as well as from a complex lipid mixture, in both low and high ionic strength buffers. It will greatly expand the accessibility of GUVs as model systems for the study of physiological processes such as membrane-binding, ion channel activity and artificial cell synthesis. Elucidation of the underlying mechanism of GUV formation will require additional studies, with emphasis on the morphological changes in the hydrated lipid films at elevated temperatures.

Acknowledgements

This work was supported by grant from the European Research Council and Swedish Science Council.

Notes and references

1 D. Lingwood and K. Simons, *Science*, 2010, **327**, 46.
2 T. Wollert, C. Wunder, J. Lippincott-Schwartz and J. H. Hurley, *Nature*, 2009, **458**, 172.
3 T. Sunami, F. Caschera, Y. Morita, T. Toyota, K. Nishimura, T. Matsuura, H. Suzuki, M. M. Hanczyc and T. Yomo, *Langmuir*, 2010, **26**, 15098.
4 K. Kurihara, M. Tamura, K.-I. Shohda, T. Toyota, K. Suzuki and T. Sugawara, *Nat. Chem.*, 2011, **3**, 775.
5 M. I. Angelova and D. S. Dimitrov, *Faraday Discuss. Chem. Soc.*, 1986, **81**, 303.
6 T. Shimanouchi, H. Umakoshi and R. Kuboi, *Langmuir*, 2009, **25**, 4835.
7 K. Tsumoto, H. Matsuo, M. Tomita and T. Yoshimura, *Colloids Surf., B*, 2009, **68**, 98.
8 K. S. Horger, D. J. Estes, R. Capone and M. Mayer, *J. Am. Chem. Soc.*, 2009, **131**, 1810.
9 P. L. Ahl, L. Chen, W. R. Perkins, S. R. Minchey, L. T. Boni and T. F. Taraschi, *Biochim. Biophys. Acta, Biomembr.*, 1994, **1195**, 237.
10 S. Pautot, B. J. Frisken and D. A. Weitz, *Langmuir*, 2003, **19**, 2870.
11 A. Yamada, M. Le Berre, K. Yoshikawa and D. Baigl, *ChemBioChem*, 2007, **8**, 2215.
12 S. Ota, S. Yoshizawa and S. Takeuchi, *Angew. Chem., Int. Ed.*, 2009, **48**, 6533.
13 D. L. Richmond, E. M. Schmid, S. Martens, J. C. Stachowiak, N. Liska and D. A. Fletcher, *Proc. Natl. Acad. Sci. U. S. A.*, 2011, **108**, 9431.
14 C. Billerit, I. Wegrzyn, G. D. M. Jeffries, P. Dommersnes, O. Orwar and A. Jesorka, *Soft Matter*, 2011, **7**, 9751.
15 D. J. Estes and M. Mayer, *Colloids Surf., B*, 2005, **42**, 115.
16 X. Han and R. W. Gross, *Biophys. J.*, 1992, **63**, 309.
17 J. Y. Lehtonen and P. K. Kinnunen, *Biophys. J.*, 1995, **68**, 525.
18 P. E. Milhiet, M.-C. Giocondi and C. Le Grimellec, *J. Biol. Chem.*, 2002, **277**, 875.
19 M. Hishida, H. Seto and K. Yoshikawa, *Chem. Phys. Lett.*, 2005, **411**, 267.
20 M. Delcea, S. Moreno-Flores, D. Pum, U. B. Sleytr and J. L. Toca-Herrera in *Biomimetics in Biophysics: Model Systems, Experimental Techniques and Computation*, ed. J. L. Toca-Herrera, Research Signpost, Kerala, 2009, p. 1.
21 H.-Z. Zhou, G. Rivas and A. P. Minton, *Annu. Rev. Biophys.*, 2008, **37**, 375.
22 L. M. Dominak and C. D. Keating, *Langmuir*, 2008, **24**, 13565.
23 K. Olbrich, W. Rawicz, D. Needham and E. Evans, *Biophys. J.*, 2000, **79**, 321.
24 J. F. Nagle and H. L. Scott, *Biochim. Biophys. Acta, Biomembr.*, 1978, **513**, 236.
25 N. A. Chebotareva, B. I. Kurganov and N. B. Livanova, *J.Biochem.*, 2004, **69**, 1239.
26 M. S. Cheung, D. Klimov and D. Thirumalai, *Proc. Natl. Acad. Sci. U. S. A.*, 2005, **102**, 4753.
27 K. Akashi, H. Miyata, H. Itoh and K. Kinosita, *Biophys. J.*, 1996, **71**, 3242.
28 M. Karlsson, K. Nolkrantz, M. J. Davidson, A. Strömberg, F. Ryttsén, B. Akerman and O. Orwar, *Anal. Chem.*, 2000, **72**, 5857.

Published on 13 September 2012 on http://pubs.rsc.org | doi:10.1039/C2SM26394G
Downloaded by Chalmers Tekniska Hogskola on 17 September 2012

 This journal is © The Royal Society of Chemistry 2012